Microchimica Acta (2023) 190:476
https://doi.org/10.1007/s00604-023-06032-2

ORIGINAL PAPER

Critical evaluation of key parameters in single particle ICP-MS data processing for the correct determination of platinum nanoparticles in complex environmental and biological matrices

Armando Sánchez-Cachero[1] · María Jiménez-Moreno[1] · Nuria Rodríguez Fariñas[1] · Rosa Carmen Rodríguez Martín-Doimeadios[1]

Received: 26 June 2023 / Accepted: 4 October 2023

Abstract
There is an urgent need for the harmonization of critical parameters in single particle inductively coupled plasma mass spectrometry (SP-ICP-MS) and they have been deeply studied and optimized in the present work using platinum nanoparticles (PtNPs) as a representative case of study. Special attention has been paid to data processing in order to achieve an adequate discrimination between signals. Thus, a comparison between four different algorithms has been performed and the method for transport efficiency calculation has also been thorougly evaluated (finding the use of a well-characterized solution of the same targeted analyte (30 nm PtNPs) as adequate). The best results have been obtained after the application of a deconvolution approach for the data processing and using 5 ms as dwell time and 40,000 data points for data acquisition. Under the optimized conditions, a correct discrimination between NP events and background signal up to 100 or 750 ng L^{-1} of added ionic Pt was reached for 30 and 50 nm PtNPs, respectively. The suitability of the developed method for the characterization of PtNPs in relevant environmental (water samples) and biological (cell culture media) matrices has also been demonstrated.

Keywords Platinum nanoparticles · Ionic platinum · Single particle inductively coupled plasma mass spectrometry · Data processing · Signal discrimination · Complex matrices

Introduction

During the last decade, single particle inductively coupled plasma mass spectrometry (SP-ICP-MS) has emerged as one of the most powerful and versatile techniques to study metallic nanoparticles (NPs) [1]. It can provide relevant analytical information both in terms of size and concentration in a particle-by-particle basis [2]. However, this technique is conditioned by several assumptions regarding data acquisition and processing that are hindering its application in routine and must be carefully considered to obtain reliable results.

Critical parameters influencing SP-ICP-MS data acquisition should be thoroughly addressed to improve signal discrimination (between NP events and background), being the most remarkable those such as dwell time, the measured data points, transport efficiency calculation, or sample dilution [3]. Working with adequate dwell time and data points will be crucial for a correct determination of the particle number concentration (PNC) and size distribution [4, 5]. Dilution can help to minimize the risk of measuring two NPs at the same time (multiple events), but if the sample is too diluted, the frequency of events would be too low and subsequently lead to long times to measure representative data sets [2, 6]. Another key parameter is the transport efficiency and the method for its calculation. Usually, it is considered to be the "Achilles heel" of this technique if traditional pneumatic aspiration is employed. By improving the transport efficiency, more reliable results will be obtained. Higher transport efficiencies also mean less time to measure representative data sets, which would be beneficial from a metrological point of view [3, 6]. Regarding this, there are several methods to calculate the transport efficiency that can be categorized into two major types, direct or indirect. The first ones are based on the use of a certified reference NP with a known PNC or size [7]. But the shortage of suitable

✉ Rosa Carmen Rodríguez Martín-Doimeadios
rosacarmen.rodriguez@uclm.es

[1] Department of Analytical Chemistry and Food Technology, Environmental Sciences Institute (ICAM), University of Castilla-La Mancha, Avda. Carlos III s/n, 45071 Toledo, Spain

Published online: 23 November 2023

certified reference NPs (stock or specifical of each NP) is a major issue for these estimations, and other novel alternatives have arisen. One of these new indirect approaches is the dynamic mass flow method proposed by the group of Goenaga-Infante [8]. It is a gravimetric approach that does not require the use of any certified NP, but is complex and time-consuming. Nevertheless, there is still a lack of consensus about how the transport efficiency can be more effectively calculated.

Another challenge that SP-ICP-MS faces is the data processing step to accurately discriminate NP signals, especially those of the smallest sizes, from the continuous background signal. Nowadays, there is no standardized method to distinguish those signals [9]. As an attempt to fill this gap, some authors have developed home-built software [10, 11] to integrate the different data processing algorithms and advance towards a harmonization of this step. Usually, threshold limits of a number of times of the standard deviation (denoted by σ) from the continuous signal have been used [12]. During the last years, σ values from 3 to 8 have been applied, but recently, 5 has been described as the best option to reduce the occurrence of false positives to virtually 0 for Poisson baseline distributions [12]. In some cases, this approach treats incorrectly background signals as NP, overestimating the number of small NPs [5]. Also, it can arbitrarily classify NP signals as background, especially in cases where more than 5σ would work better as threshold [12, 13]. The setting of threshold limits based on outlier analysis seems to introduce a bias, especially, for challenging situations, when overlap between signals may occur, such as the analysis of complex samples. In these cases, the use of a deconvolution approach [14] appears to be more suitable. This method is based on the fitting of polyagaussian probability mass functions to frequencies of the lowest signal intensities such as those of blanks or dissolved ions and the subsequent subtraction of the dissolved signal component. Another alternative is to apply a *K*-clustering algorithm, proposed by Bi et al. [15], which defines groups in the data set based on their similarity [15]. This approach needs the optimization of the *K* value for each situation, which is crucial for an optimum discrimination, making this option arduous to perform [15]. Therefore, the performance of reliable studies of NPs in complex matrices using SP-ICP-MS is still an arduous task due to the lack of harmonization for the data acquisition and processing conditions, and a thorough optimization would be needed.

Thus, this work is devoted to the development and critical evaluation of an analytical method based on SP-ICP-MS for the correct characterization and quantification of NPs in terms of size distribution, and PNC. As a case study, platinum nanoparticles (PtNPs) have been investigated due to their interesting properties for many biomedical [16], technological, and daily product applications, which come with an increase of their release into the environment and the subsequential human exposure [17]. Different methods for data processing based on distinct algorithms have been rigorously evaluated and compared. Also, key acquisition parameters, such as dwell time, data points, dilution effect, and the method for the calculation of the transport efficiency, have been thoroughly optimized. Additionally, the applicability of the optimized method for the discrimination between ionic and NP forms of Pt under co-existence conditions and the characterization of PtNPs in relevant environmental and biological matrices have been addressed.

Materials and methods

Chemical and reagents

All chemicals and reagents were of analytical grade. Solutions were prepared in ultrapure water (18.2 MΩ•cm), obtained from a Milli-Q® A10™ water purification system (Millipore Corporation, USA). Details of all reagents are given in the Electronic Supporting Material (ESM, Supplementary text, Section 1).

Commercial solutions of 30 and 50 nm PtNPs and 30 nm AuNPs stabilized in 2 mM citrate were purchased from nanoComposix (USA). Characterization of those solutions is provided in the ESM (Supplementary text, Section 2). Before their use, all NP solutions were homogenized for 1 min with vortex agitation (using an advanced ZX3 Vortex from Velp Scientifica, Italy) at 1200 rpm to prevent NP aggregation. Then, they were diluted to accomplish the SP-ICP-MS requirements stated in previous works [4, 13, 18]. Also, more challenging situations which exceed these typical working conditions were considered.

SP-ICP-MS analysis: instrumental conditions and data processing

A triple quadrupole ICP-MS iCap-TQ (Thermo Electron Corporation, Germany), equipped with a Micromist nebulizer and a cyclonic spray chamber, was employed for SP-ICP-MS analysis. Operational conditions are summarized in Table 1. The equipment was tuned daily for the highest sensitivity in the Single Quadrupole Kinetic Energy Discrimination (SQ-KED) mode with He as collision gas. Raw signal data were processed using different methods and algorithms by means of the npQuant plug-in of Qtegra™ Intelligent Scientific Data Solution™ (ISDS) and Nanocount version 3.2 software [11] to obtain the size distribution and PNC. These calculations were performed using the density of Pt and mass fraction of PtNPs and assuming that NPs are spherical and solid. The data of a particle solution (30 nm PtNPs with a nominal size of 32 ± 3 nm at $5.28 \cdot 10^4$ p mL^{-1})

Table 1 SP-ICP-MS operating conditions

RF-Power (KW)	1.5
Plasma gas flow rate (L min^{-1})	14
Carrier gas flow rate (L min^{-1})	1
Nebulizer flow rate (L min^{-1})	1.0
Auxiliary gas flow rate (L min^{-1})	0.8
Nebulizer	Meinhard type
Spray chamber	Cyclonic type
Isotope monitored	^{195}Pt
Analyte mass (u.m.a)	194.96
Density (g cm^{-3})	21.45
Mode	SQ-KED
He flow rate (mL min^{-1})	4.9
Q1 bias (V)	− 2.5
Qcell bias (V)	− 2.0
Q3 bias (V)	− 1.0
Transport efficiency (%)	9–12
Sample flow rate (mL min^{-1})	0.32–0.40
Dwell time (ms)	5
Acquisition time (s)	200
Data points	40,000

was used in each series of measurements as a reference to determine the transport efficiency and for the calculations of particle size and concentrations. The response factor of the ionic analyte standard must also be known and was calculated using different standards (100 to 2000 ng L^{-1}) of ionic Pt. The sample flow rate was estimated daily by measuring the mass of water taken up by the instrument for 5 min. This measurement was performed by duplicate. The concentration and size limit of detection (LOD_c and LOD_{size}, respectively) were calculated using the spreadsheet proposed by Laborda et al. [12]. Particle events in corresponding blanks were measured and subtracted through all the experiments.

Sample preparation

Synthetic water referred to as moderately hard water was prepared following a U.S. Environmental Protection Agency protocol (EPA-821-R-02–12) [19], in the presence (2 mg L^{-1}) or absence of humic acid (HA). Chemical composition and characterization are provided in Table S1. Tap water sample was taken from our laboratory after letting flow for 5 min. Two different water samples (W#1 and W#2) were collected in locations along the Tagus River in Castilla, La Mancha region, Spain. Global positioning system (GPS) coordinates and water characteristics are presented in Table S2.

For the experiments with cell culture media, Dulbecco's modified eagle medium (DMEM)-high glucose was used either directly or supplemented with a mixture of antibiotics (100 U mL^{-1} of penicillin and 100 µg mL^{-1} streptomycin) or a combination of these antibiotics with 10% of fetal bovine serum (FBS).

A series of dilutions ($3.02•10^4$–$1.06•10^5$ p mL^{-1}) of 30 nm PtNPs were mixed in each of the studied matrices (water samples and cell culture media) in the absence or presence of different reagents (2% HCl, 0.1% cysteine (Cys), or a mixture of them). In all cases, samples were homogenized by vortex agitation for 10 s.

Results and discussion

During the optimization process of this SP-ICP-MS-based method, critical parameters have been meticulously addressed for an accurate determination of PtNP size distribution (nm) and PNC (p mL^{-1}) with a special focus on data processing. Recoveries (%) were calculated as the found PNC relative to the spiked PNC.

Comparison of data processing algorithms

Dilution is an important factor when working with this technique because if samples are not sufficiently or too diluted, size and concentrations would be determined in a wrong way. There are two potential scenarios that would respond to different statistical distributions. On one hand, the frequency distribution of samples with low-intensity signals will follow a Poisson distribution [2, 4]. Some authors recommend selecting the dilution based on a ratio between the desired NP events in the plasma and the number of total data points [4, 13, 18]. Commonly, under well-established data processing conditions (such as the 5-σ criterion), it is accepted that a ratio of 0.1 is enough for an adequate size determination, but to obtain reliable PNC results, this ratio has to be 0.05 [13, 18]. On the other hand, if samples have a high dissolved or particle concentration (or both combined), their frequency distribution will follow a Polyagaussian distribution; other data processing conditions that attend to this particular issue should be applied, such as the deconvolution approach [14]. Thus, in order to cover both scenarios, samples containing 30 or 50 nm PtNPs individually were diluted in ultrapure water covering a range from $1.06•10^4$ to $3.02•10^5$ p mL^{-1} through all the experiments (which corresponds to ratios from ≈ 0.03 to 0.75, calculated taking an average value of transport efficiency of $10 \pm 0.4\%$ ($n = 6$)). Regarding the data acquisition, 5 ms was initially established as dwell time (based on previous studies with PtNPs [20]), and the number of data points used was 30,000, until their optimization in ESM (Supplementary text, Section 3). Under these conditions, samples can be divided into two main groups, the ones that will match Poisson statistics ($1.06•10^4$ to $5.28•10^4$ p

mL^{-1}) and those with higher intensities that will follow a Polyagaussian distribution ($1.06•10^5$ to $3.02•10^5$ p mL^{-1}).

Four different algorithms to discriminate between PtNPs and the background signal to obtain information on size and concentration have been tested. Thus, the proprietary software of the ICP-MS instrument (npQuant plug-in from Thermo Electron Corporation), a well-established approach (5-σ criterion) [12], an option based on *K*-clustering algorithm [15], and a deconvolution method stated by Cornelis et al. (2014) [11, 14] have been compared. Their performance to determine recovery (%) using the initial acquisition conditions mentioned above has been tested. The mean registered particle events in three consecutive blanks ($n=3$) were measured and calculated for each case. Thus, the false positives arising from the background signal were subtracted. Obtained recoveries using the software npQuant for 30 nm PtNPs (Fig. 1A) were lower as long as the PtNP concentration raises. But, for 50 nm PtNPs (Fig. 1B), this decrease is not noticeable up to samples above the Poisson requirements ($5.28•10^4$ p mL^{-1}). This software works with pre-fixed upper and lower thresholds, which are selected based on the frequency distribution of a reference NP. This fact can explain the low recoveries for most dilutions since it is not able to resolve changes in the frequency distribution.

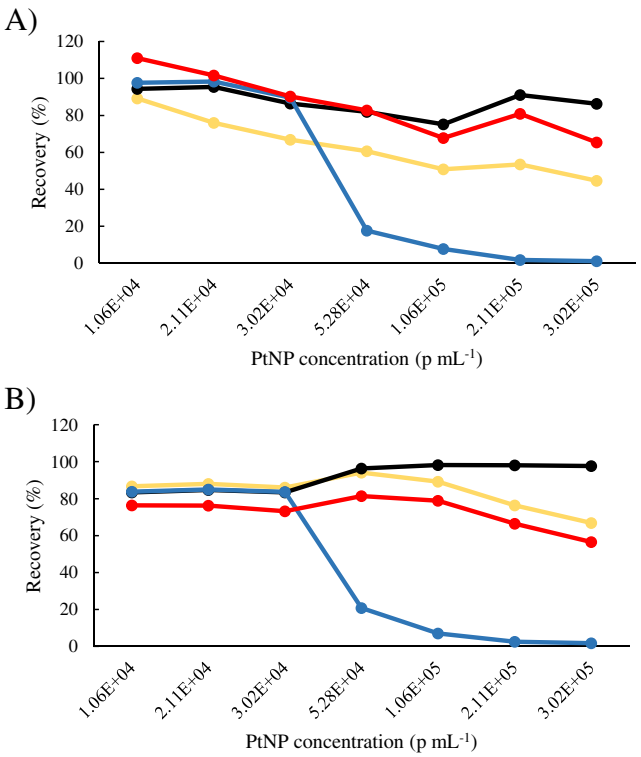

Fig. 1 Recoveries (%) for PtNP PNC (p mL^{-1}) of **A** 30 nm and **B** 50 nm PtNPs using 5-σ criterion (blue), *K*-means (red), npQuant (yellow), and deconvolution (black) as data processing method (5 ms as dwell time, and 30,000 data points for data acquisition)

When the 5-σ criterion and high PtNP concentrations were used, the signal discrimination was very poor, obtaining a high percentage of false negatives. In this case, a correct signal discrimination was only achieved in a short range of concentrations ($1.06•10^4$ – $3.02•10^4$ p mL^{-1}) for both PtNP sizes, since those samples will follow Poisson statistics correctly. Applying *K*-means ($K=2$) results in a constant decreasing trend of the recoveries when the concentration raises consistent with that observed for npQuant. Close to 100% recoveries were obtained for 30 nm (Fig. 1A) mainly at higher dilutions, but for 50 nm (Fig. 1B), they were close to 80% until the concentration raises above $1.06•10^5$ p mL^{-1}. In the present work, $K=2$ has been selected taking into account the literature [15]. This algorithm classifies signals based on their similarity, specifically into *K* groups with *K* centers (each center corresponding to a single group). Therefore, in an ideal situation, where only 2 groups are present in the sample (NP signals and background), 2 is selected as the *K* value. However, this assumes a monodisperse NP solution, which is rarely the case. Thus, in a real situation like the one studied, part of the particle distribution is going to be addressed as background signals, causing an inaccurate signal discrimination. Lastly, when the deconvolution algorithm was applied, recoveries close to 100% were reported in a wider range of PtNP concentrations (Fig. 1A and B). Even though values achieved for PtNP sizes applying this algorithm were adequate, the ones obtained for 50 nm PtNPs were higher. This can be explained by its frequency distribution, which would be easily deconvolved from the dissolved one as it is located further from the background signal distribution being less overlapped.

For SP-ICP-MS analysis, not only a correct concentration determination should be achieved, but also size distribution must be accurately determined. Regarding particle size determination (Figure S1), when the software from the instrument is used, the calculated size remained almost constant for the two studied PtNP sizes (Figures S1A and B). Therefore, if changes in the frequency distribution are not resolved, the size seems to be not greatly disturbed. If 5-σ is applied as a data processing method, more biased results are obtained. In this case, size was correctly determined for both sizes in the same short range of concentrations ($1.06•10^3$–$3.02•10^4$ p mL^{-1}). Size determination under the *K*-means algorithm was adequate for 30 nm PtNPs (Figure S1A) in all cases, but for 50 nm PtNPs (Figure S1B), it was overestimated. As explained earlier, the subjectiveness introduced by selecting this *K* value can produce the observed effects, as it can change completely particle size distribution. For deconvolution, following the same tendency observed for concentrations, size was accurately determined through all the concentrations studied.

In order to compare the performance of the different employed algorithms, the linearity was calculated, along

with the LOD_{size} and LOD_c (Table 2). Deconvolution offers a wider linearity range since it can work with samples above the Poisson requirements [14]. Regarding LOD_{size} and LOD_c, there is no method to accurately calculate them using deconvolution or *K*-means, so they were calculated following the definitions proposed by Laborda et al. (2020) for other data processing algorithms [12]. Even though lower values were achieved using deconvolution, significant differences were not found between them. As mentioned above, other data processing methods, like 5-σ criterion or *K*-means, can perform an accurate size and PNC but in a narrower range than deconvolution, probably because those works were conducted under samples following Poisson statistics and also because of the subjective bias that an outlier analysis introduces in the data processing, making the dilution range a restrictive condition for an SP-ICP-MS analysis. Thus, by using deconvolution, the dynamic concentration range where those parameters are correctly studied can be expanded, since it offers a better discrimination when the overlapping of signals occurs [14].

Transport efficiency calculation method

The feasibility of the SP-ICP-MS analysis relies on the transport efficiency calculation. Therefore, the correct estimation of this parameter becomes crucial. As a rule of thumb, a direct method based on the size of AuNP reference standards [7], such as NIST RM 8011, 8012, and 8013 or LGC QC5050, has been used for transport efficiencies calculations for a variety of metallic NPs including PtNPs [6, 9, 21–24]. But the limited availability of an adequate reference NP made this direct approach challenging. Moreover, this method based on a standard NP relies on the element sensitivity as one of the parameters to do the calculations, so it would be of paramount interest to use NP reference materials of the same element, since differences between elements' sensitivities are usually reported [4, 9]. Therefore, a well-characterized NP with the same core as the target NP appears to be the most convenient direct approach for that task.

Table 2 PNC linear range (p mL^{-1}), concentration, and size limits of detection (LOD) for the studied data processing algorithms

Algorithm	PNC linear range	LOD_{size} (nm)	LOD_c (μg L^{-1})
NP-Quant[1]	$1.06•10^4$ to $2.11•10^5$	17.16	0.063
5-σ criterion[2]	$1.06•10^4$ to $3.02•10^4$	16.95	0.077
K-means[3]	$1.06•10^4$ to $1.06•10^5$	17.01	0.066
Deconvolution[4]	$1.06•10^4$ to $3.02•10^5$	16.70	0.059

[1]Software from Thermo Electron Corp

[2]Refs. [7] and [12]

[3]Ref. [15]

[4]Ref [14]

After a study of other acquisition parameters, such as dwell time and data points (ESM, Supplementary text, Section 3), where 5 ms and 40,000 data points were found as optimum, different methods for the estimation of transport efficiency have been compared. This parameter was calculated using either a solution of 30 nm PtNPs purchased at nanoComposix (32 ± 3 nm) or the LGC QC5050 AuNPs standard (33 ± 2 nm). A novel gravimetric method, which is based on indirect assumptions and does not need the use of any reference NP, has also been tested (Table S3) [8]. No remarkable differences were observed between the transport efficiencies (Table S3) obtained using the distinct approaches. It involves that no statistically significant differences were found ($p < 0.05$) in the determination of PtNP size and concentration when applying the different values (Table S3).

As previously stated, transport efficiency calculations are based on many assumptions (e.g., element density and sensitivity, or the certified size) [7]. Accordingly, to reduce the uncertainty (or assumed error) on those calculations and improve the transport efficiency values and the simplicity of the analysis routine, the use of a NP made from the same element that the targeted analyte (Pt in this case) as reference appears to be beneficial. Therefore, we suggest this option while appropriate certified materials with known particle size are available. Regarding the application of the indirect approach, its use can be suitable to calculate the transport efficiency in situations where certified reference materials are lacking [8]. However, this method is time-consuming and arduous to perform, so it can be mainly considered a control tool to check the accuracy of the determined size of a NP solution before being used as a reference for the other methods.

Even so, all transport efficiencies obtained were below 15%. This is a typical drawback for SP-ICP-MS methodologies if traditional aspiration based on regular-flow nebulizers and cyclonic spray chambers is employed [6]. Due to technological limitations, the improvement of this value can just be achieved if other aspiration devices are used. In this sense, there are several alternatives based on pneumatic nebulization such as microdroplet generator or total consumption chambers, where values close to 100% can even be reached that can be explored [25].

Study of discrimination capabilities

Final optimized SP-ICP-MS operating conditions are summarized in Table 1. As a proof of applicability for the discrimination of different NP sizes, mixtures of 30 and 50 nm

PtNPs at different concentrations ($1.06•10^4$–$1.06•10^5$ p mL^{-1} for each NP) were analyzed using deconvolution as a data processing algorithm, providing an accurate size and concentration determination of both PtNPs. As an example, the frequency histogram after the deconvolution treatment as well as the final particle size distribution of a mixture of 30 and 50 nm PtNPs at intermediate concentrations ($5.28•10^4$ p mL^{-1} for each NP) is shown in Figure S6.

One of the main goals of the SP-ICP-MS method is to achieve a correct discrimination of ionic (or dissolved) and NP signals, since both forms can co-exist, and the performance of the analysis should not be affected by this fact. In this regard, the developed method was tested under situations where this discrimination between signals can be difficult, leading to errors in the determination of the concentration and size. For that aim, two sizes of PtNPs (30 and 50 nm) were mixed individually (≈ $5•10^4$ p mL^{-1}) or jointly with increasing concentrations of ionic Pt (0–4000 ng L^{-1}). Regarding concentration (Fig. 2), quantitative recoveries were obtained up to 100 ng L^{-1} of ionic Pt for 30 nm and 750 ng L^{-1} for 50 nm and the mixture of both PtNP sizes. Larger dissolved concentrations in each situation lead to underestimation in the concentration, being most of the PtNPs regarded as ionic signals.

The higher value for 50 nm and the mixture can be attributed to the higher intensity frequencies that are needed to produce signal overlapping. Size was accurately determined (Figure S7) for a larger range of added ionic Pt concentrations even though concentration was not correctly determined in some of these cases. For 30 nm, size was overestimated when more than 500 ng L^{-1} of ionic Pt is added, alone (Figure S7A) or mixed with 50 nm PtNPs (Figure S7B). For 50 nm, size was overestimated when these NPs were mixed with 1500–2000 ng L^{-1} of ionic Pt (Figure S7A). For the mixture sample (30 and 50 nm PtNPs simultaneously), a misleading determination was obtained, since, apparently, no overestimation was observed until 3000 ng L^{-1} of ionic Pt (Figure S7B). However, this is caused by an overestimation of the 30 nm PtNP distribution, which is incorrectly determined as 50 nm PtNPs.

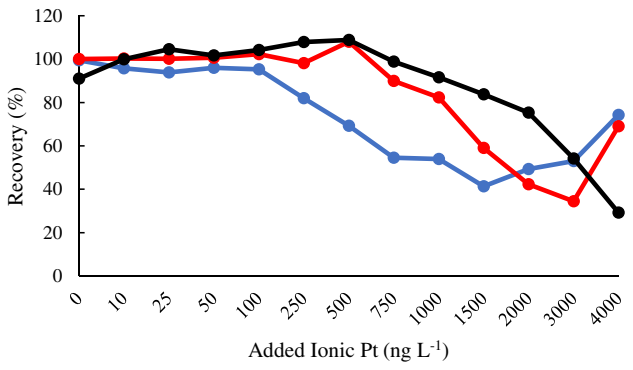

Fig. 2 Recoveries (%) of PtNPs at increasing ionic platinum concentrations for 30 (blue), 50 nm (red) PtNPs, or a mixture of both PtNPs (black) at a concentration of ≈ $5•10^4$ p mL^{-1} each

Hence, it has been demonstrated that this method can be applied to follow size changes under situations where high ionic Pt is expected to be present, although under these conditions it can be limited for the accurate calculation of concentration.

Analytical characterization of the method

Working under the optimized data acquisition (Table 1) and deconvolution as data processing, a full analytical performance characterization of the method has been carried out for 30 nm PtNPs. The studied characteristics for PNC ($5.28•10^4$ p mL^{-1}) and size were trueness (referred as the closeness of agreement between the determined mean and the reference or expected values, %), intra-day precision (relative standard deviation in six replicates measured in the same day, RSD_{intra}), inter-day precision (relative standard deviation in samples measured in six different days, RSD_{inter}), and linearity (studied in a range between $1.06•10^4$ and $3.02•10^5$ p mL^{-1}). All results are summarized in Table 3. Trueness close to 100% for concentration and particle size was achieved when comparing the found and expected values, demonstrating the accuracy of the analysis. With respect to the precision, values below 2% for concentration and below 1% for size were found for intra- and inter-day precisions, respectively. In the same way, good linearity was reported in the studied range for concentration (as represented in the scatterplot, Figure S8). As presented earlier, low size (13.78 nm) and concentration (0.029 ng L^{-1}) of LODs were reached. Nevertheless, to perform a complete analytical validation process, it would be required the existence of PtNP reference materials, which are not currently available.

Determination of PtNPs in environmental and biological matrices

As stated earlier, PtNPs are present in almost all environmental compartments and organisms, and therefore, their

Table 3 Analytical characteristics of the optimized SP-ICP-MS method in terms of mass concentration and size for trueness (expressed as mean and standard deviation ($n=6$)), intra-day precision (RSD_{intra}), and inter-day precision (RSD_{inter}) for PtNPs (32 ± 3 nm at $5.28•10^4$ p mL^{-1})

	Mass concentration	Size
Trueness (%)	94 ± 8	100 ± 7
RSD_{intra} (%)	1.8	0.7
RSD_{inter} (%)	1.9	0.9

monitoring would be interesting [26]. Up to now, SP-ICP-MS has been mainly used to study PtNPs in environmental samples, such as synthetic waters [22], road dust [27], or plants [23], although some application to biofluids has also been reported [20].

The applicability of the optimized method for the determination of PtNPs in complex biological samples has been evaluated in the present work using DMEM (directly, supplemented only with antibiotics, or with antibiotics and 10% FBS). Also, it has been tested in moderately hard water (Table S1) without and with 2 mg L^{-1} of HA, as an example of a proposed media for ecotoxicity tests involving nanomaterials [28] and three real water samples (tap water and two collected in the Tagus River, W #1–2, characterization in Table S2). The effect over concentration and size of different reagents previously used in the literature has been tested. Cysteine was selected based on other studies where it was employed to reduce the memory and matrix effects, improving the LODs of other metals using ICP-MS-based techniques [14]. In the same way, HCl has been typically used in environmental and biological analysis to reduce the matrix effect and improve sensitivities [3]. Therefore, for this study, 30 nm PtNPs (at $5.28 \bullet 10^4$ p Ml^{-1}) were mixed with 2% HCl, 0.1% Cys, or a mixture of both, in each matrix.

For DMEM, there were no major size changes in the core size under any circumstances (Figure S9A). It can be related to the potential formation of a "bio-corona," which typically occurs to NPs in this kind of matrices that may have conferred more stability to the PtNPs than their own coating, preventing the core from any clustering processes [29]. The formation of this interaction was reported for a variety of NPs in various biological matrices [30, 31]. As for PtNPs, it has been previously studied by Fernández-Trujillo et al. [20] in the same cell culture media by means of HPLC-ICP-TQ-MS, where it was immediately observed. As a result of the formation of the bio-corona, growth in the hydrodynamic diameters of PtNPs was reported, but aggregates, agglomerates, or relevant changes in their diameters were not observed using HR-SEM or DLS [32]. Regarding concentration determination (Figure S10A), no statistically significant differences were found ($p < 0.05$).

In contrast, interesting transformations have been observed in other matrices such as synthetic waters. Samples with cysteine (0.1% or mixture with HCl) experienced growth on the mean determined diameter (Figure S9B). The formation of larger aggregates can be responsible for this increase, as it can be checked regarding particle size distributions (Fig. 3).

In moderately hard water, those aggregates were only formed in samples with cysteine (Fig. 3A). This effect is also accompanied with a decrease in the concentration for 30 nm PtNP peak (Figure S10B). However, when organic matter (2 mg L^{-1} of HA) is added, those effects are diminished

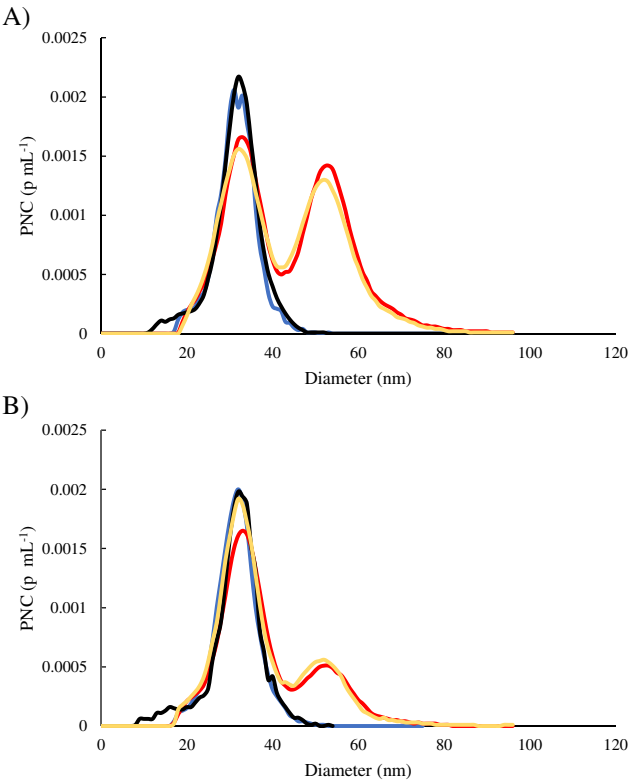

Fig. 3 Particle size distribution in the presence of 2% HCl (blue), 0.1% Cys (red), a mixture of both (yellow), or none (black) for 30 nm PtNPs ($5 \bullet 10^4$ p mL^{-1}) in moderately hard water **A** without or **B** with (2 mg L^{-1}) humic acid (HA)

(Fig. 3B), reducing the growth in the mean diameter and the concentration decrease. In this situation, a comparable effect to the one reported in biological matrices seems to be happening. The interaction of the organic matter with the PtNPs results in the formation of an "eco-corona," which also enhances their stability. This is a common transformation for NPs in the environment, being reported in various studies [33, 34]. Specifically for different sized PtNPs, the formation of this coating was also described in a previous work using AF4-ICP-MS, where the interaction of organic matter in synthetic waters was studied following changes in their hydrodynamic diameters [35]. Thus, when organic matter was present, aggregation was reduced, while their hydrodynamic diameters increased. Organic matter can either replace or overcoat PtNPs' original coating, which ultimately increases their stability [35].

Finally, the proposed method was tested under real environmental conditions. PtNPs were spiked in tap water and two samples collected in the Tagus River (W #1 and #2). No differences on the average determined diameter were reported under any circumstances (Figure S9C) even though conductivity and hardness in the river waters are higher (Table S2) than in the synthetic water (Table S1).

This can be explained through the formation of the "eco-corona" as previously observed in the synthetic water with organic matter. In all these samples, natural organic matter is present, which can result in the formation of the same entity, preventing any aggregation process. As for concentration (Figure S10C), no relevant differences were observed, following the same tendency as in previous samples.

Conclusions

The proposed method based on SP-ICP-MS using an underexploited deconvolution algorithm for data processing has been efficient to follow changes and transformations of PtNPs in relevant environmental and biological matrices, which would be interesting for toxicological and environmental fate studies. Although PtNPs have been used in this study, the method shows great potential to be applied to other metallic NPs, since all the conditions are still general and not restricted or conditioned by Pt or the reference solution used for the transport efficiency calculations. In this sense, this approach can be used as a tool to assess other NPs in complex biological and environmental matrices.

The results of this work also highlight the need for a deep understanding of crucial SP-ICP-MS parameters and concepts, to reach harmonized methodologies or strategies to correctly perform any analysis using this approach. Also, there is an imperative necessity for the development and production of adequate reference materials for NP analysis, with certified size and mass- and number-based concentration values. Thus, further research and inter-laboratory comparisons would be helpful in the advancement of this technique's maturity.

Supplementary Information The online version contains supplementary material available at https://doi.org/10.1007/s00604-023-06032-2.

Funding The authors would like to thank the Spanish Ministerio de Ciencia e Innovación and Junta de Comunidades Castilla-La Mancha for supporting this work through the projects PID2022-138761NB-I00 and SBPLY/21/180501/000188, respectively.

Data availability The data that support the findings of this study are available from the corresponding author upon reasonable request.

Declarations

Conflict of interest The authors declare no competing interests.

References

1. Bolea E, Jimenez MS, Perez-Arantegui J et al (2021) Analytical applications of single particle inductively coupled plasma mass spectrometry: a comprehensive and critical review. Anal Methods 13:2742–2795. https://doi.org/10.1039/D1AY00761K
2. Laborda F, Bolea E, Jiménez-Lamana J (2014) Single particle inductively coupled plasma mass spectrometry: a powerful tool for nanoanalysis. Anal Chem 86:2270–2278. https://doi.org/10.1021/ac402980q
3. Montaño MD, Olesik JW, Barber AG et al (2016) Single Particle ICP-MS: advances toward routine analysis of nanomaterials. Anal Bioanal Chem 408:5053–5074. https://doi.org/10.1007/s00216-016-9676-8
4. Olesik JW, Gray PJ (2012) Considerations for measurement of individual nanoparticles or microparticles by ICP-MS: determination of the number of particles and the analyte mass in each particle. J Anal At Spectrom 27:1143. https://doi.org/10.1039/c2ja30073g
5. Tuoriniemi J, Cornelis G, Hassellöv M (2012) Size discrimination and detection capabilities of single-particle ICPMS for environmental analysis of silver nanoparticles. Anal Chem 84:3965–3972. https://doi.org/10.1021/ac203005r
6. Resano M, Aramendía M, García-Ruiz E et al (2022) Living in a transient world: ICP-MS reinvented *via* time-resolved analysis for monitoring single events. Chem Sci 13:4436–4473. https://doi.org/10.1039/D1SC05452J
7. Pace HE, Rogers NJ, Jarolimek C et al (2011) Determining transport efficiency for the purpose of counting and sizing nanoparticles via single particle inductively coupled plasma mass spectrometry. Anal Chem 83:9361–9369. https://doi.org/10.1021/ac201952t
8. Cuello-Nuñez S, Abad-Álvaro I, Bartczak D et al (2020) The accurate determination of number concentration of inorganic nanoparticles using spICP-MS with the dynamic mass flow approach. J Anal At Spectrom 35:1832–1839. https://doi.org/10.1039/C9JA00415G
9. Minelli C, Wywijas M, Bartczak D et al (2022) Versailles project on advanced materials and standards (VAMAS) interlaboratory study on measuring the number concentration of colloidal gold nanoparticles. Nanoscale 14:4690–4704. https://doi.org/10.1039/D1NR07775A
10. Peters R, Herrera-Rivera Z, Undas A et al (2015) Single particle ICP-MS combined with a data evaluation tool as a routine technique for the analysis of nanoparticles in complex matrices. J Anal At Spectrom 30:1274–1285. https://doi.org/10.1039/C4JA00357H
11. Cornelis G (2022) Nanocount (version 3.2), Swedish Agricultural Sciences University. Available: https://blogg.slu.se/nanocount/. Accessed 11 July 2023
12. Laborda F, Gimenez-Ingalaturre AC, Bolea E, Castillo JR (2020) About detectability and limits of detection in single particle inductively coupled plasma mass spectrometry. Spectrochim Acta Part B At Spectrosc 169:105883. https://doi.org/10.1016/j.sab.2020.105883
13. Kaynarova LI, Georgieva DL, Stefanova VM (2022) An approach to estimate the contribution of signal noise to the diameter uncertainty of individual silver nanoparticles and resolution of spICP-MS analysis. J Anal At Spectrom 37:1484–1500. https://doi.org/10.1039/d2ja00039c
14. Cornelis G, Hassellöv M (2014) A signal deconvolution method to discriminate smaller nanoparticles in single particle ICP-MS. J Anal At Spectrom 29:134–144. https://doi.org/10.1039/C3JA50160D
15. Bi X, Lee S, Ranville JF et al (2014) Quantitative resolution of nanoparticle sizes using single particle inductively coupled plasma mass spectrometry with the K-means clustering algorithm. J Anal At Spectrom 29:1630–1639. https://doi.org/10.1039/c4ja00109e
16. Jeyaraj M, Gurunathan S, Qasim M et al (2019) A comprehensive review on the synthesis, characterization, and biomedical

application of platinum nanoparticles. Nanomaterials 9:1719. https://doi.org/10.3390/nano9121719
17. Bundschuh M, Filser J, Lüderwald S et al (2018) Nanoparticles in the environment: where do we come from, where do we go to? Environ Sci Eur 30:6. https://doi.org/10.1186/s12302-018-0132-6
18. Laborda F, Jiménez-Lamana J, Bolea E, Castillo JR (2013) Critical considerations for the determination of nanoparticle number concentrations, size and number size distributions by single particle ICP-MS. J Anal At Spectrom 28:1220–1232. https://doi.org/10.1039/c3ja50100k
19. U.S. E.P.A. (2002) Methods for measuring the acute toxicity of effluents and receiving waters to freshwater and marine organisms, 5th edn. Washington D.C., EPA-821-R-02-12. Available: https://www.epa.gov/sites/default/files/2015-08/documents/acute-freshwater-and-marine-wet-manual_2002.pdf. Accessed 11 July 2023
20. Fernández-Trujillo S, Jiménez-Moreno M, Ríos Á, del Carmen Rodríguez Martín-Doimeadios R (2021) A simple analytical methodology for platinum nanoparticles control in complex clinical matrices via SP-ICP-MS. Talanta 231:122370. https://doi.org/10.1016/j.talanta.2021.122370
21. Sikder M, Wang J, Chandler GT et al (2019) Synthesis, characterization, and environmental behaviors of monodispersed platinum nanoparticles. J Colloid Interface Sci 540:330–341. https://doi.org/10.1016/j.jcis.2019.01.036
22. Sikder M, Wang J, Poulin BA et al (2020) Nanoparticle size and natural organic matter composition determine aggregation behavior of polyvinylpyrrolidone coated platinum nanoparticles. Environ Sci Nano 7:3318–3332. https://doi.org/10.1039/D0EN00659A
23. Jiménez-Lamana J, Wojcieszek J, Jakubiak M et al (2016) Single particle ICP-MS characterization of platinum nanoparticles uptake and bioaccumulation by Lepidium sativum and Sinapis alba plants. J Anal At Spectrom 31:2321–2329. https://doi.org/10.1039/C6JA00201C
24. Geiss O, Bianchi I, Bucher G et al (2022) Determination of the transport efficiency in spICP-MS analysis using conventional sample introduction systems: an interlaboratory comparison study. Nanomaterials 12:725. https://doi.org/10.3390/nano12040725
25. Lin F, Miyashita S, Inagaki K et al (2019) Evaluation of three different sample introduction systems for single-particle inductively coupled plasma mass spectrometry (spICP-MS) applications. J Anal At Spectrom 34:401–406. https://doi.org/10.1039/C8JA00295A
26. Nejdl L, Kudr J, Blazkova I et al (2015) Platinum metals in the environment. Springer, Berlin Heidelberg, Berlin, Heidelberg
27. Folens K, van Acker T, Bolea-Fernandez E et al (2018) Identification of platinum nanoparticles in road dust leachate by single particle inductively coupled plasma-mass spectrometry. Sci Total Environ 615:849–856. https://doi.org/10.1016/j.scitotenv.2017.09.285
28. Geitner NK, Ogilvie Hendren C, Cornelis G et al (2020) Harmonizing across environmental nanomaterial testing media for increased comparability of nanomaterial datasets. Environ Sci Nano 7:13–36
29. García-Álvarez R, Vallet-Regí M (2021) Hard and soft protein corona of nanomaterials: analysis and relevance. Nanomaterials 11:888. https://doi.org/10.3390/nano11040888
30. Soto-Alvaredo J, López-Chaves C, Sánchez-González C et al (2017) Speciation of gold nanoparticles and low-molecular gold species in Wistar rat tissues by HPLC coupled to ICP-MS. J Anal At Spectrom 32:193–199. https://doi.org/10.1039/C6JA00248J
31. López-Sanz S, Rodríguez Fariñas N, Rodríguez M-D, C, Ríos Á, (2019) Analytical strategy based on asymmetric flow field flow fractionation hyphenated to ICP-MS and complementary techniques to study gold nanoparticles transformations in cell culture medium. Anal Chim Acta 1053:178–185. https://doi.org/10.1016/j.aca.2018.11.053
32. Fernández-Trujillo S, Rodríguez Fariñas N, Jiménez-Moreno M, Rodríguez Martín-Doimeadios RC (2021) Speciation of platinum nanoparticles in different cell culture media by HPLC-ICP-TQ-MS and complementary techniques: a contribution to toxicological assays. Anal Chim Acta 1182:338935. https://doi.org/10.1016/j.aca.2021.338935
33. Baalousha M, Afshinnia K, Guo L (2018) Natural organic matter composition determines the molecular nature of silver nanomaterial-NOM corona. Environ Sci Nano 5:868–881. https://doi.org/10.1039/C8EN00018B
34. Fischer J, Gräf T, Sakka Y et al (2021) Ion compositions in artificial media control the impact of humic acid on colloidal behaviour, dissolution and speciation of CuO-NP. Sci Total Environ 785:147241. https://doi.org/10.1016/j.scitotenv.2021.147241
35. Sánchez-Cachero A, López-Sanz S, Rodríguez Fariñas N et al (2021) A method based on asymmetric flow field flow fractionation hyphenated to inductively coupled plasma mass spectrometry for the monitoring of platinum nanoparticles in water samples. Talanta 222:121513. https://doi.org/10.1016/j.talanta.2020.121513